

# Relevance of the Fanconi anemia pathway in the response of human cells to trabectedin

José A. Casado,<sup>1</sup> Paula Río,<sup>1</sup> Esther Marco,<sup>2</sup> Verónica García-Hernández,<sup>3</sup> Alberto Domingo,<sup>3</sup> Laura Pérez,<sup>1,5</sup> Juan Carlos Tercero,<sup>5</sup> Juan José Vaquero,<sup>4</sup> Beatriz Albella,<sup>1</sup> Federico Gago,<sup>2</sup> and Juan A. Bueren<sup>1</sup>

<sup>1</sup>Division of Hematopoiesis and Gene Therapy Program, Centro de Investigaciones Energéticas, Medioambientales y Tecnológicas and Centro de Investigación Biomédica en Red de Enfermedades Raras; Departments of <sup>2</sup>Pharmacology, <sup>3</sup>Biochemistry and Molecular Biology, and <sup>4</sup>Organic Chemistry, Universidad de Alcalá, Alcalá de Henares; and <sup>5</sup>PharmaMar S.A., Madrid, Spain

## Abstract

Trabectedin (Yondelis; ET-743) is a potent anticancer drug that binds to DNA by forming a covalent bond with a guanine in one strand and one or more hydrogen bonds with the opposite strand. Using a fluorescence-based melting assay, we show that one single trabectedin-DNA adduct increases the thermal stability of the double helix by >20°C. As deduced from the analysis of phosphorylated H2AX and Rad51 foci, we observed that clinically relevant doses of trabectedin induce the formation of DNA double-strand breaks in human cells and activate homologous recombination repair in a manner similar to that evoked by the DNA interstrand cross-linking agent mitomycin C (MMC). Because one important characteristic of this drug is its marked cytotoxicity on cells lacking a functional Fanconi anemia (FA) pathway, we compared the response of different subtypes of FA cells to MMC and trabectedin. Our data clearly show that human cells with mutations in *FANCA*, *FANCC*, *FANCF*, *FANCG*, or *FANCD1* genes are highly sensitive to both MMC and trabectedin. However, in marked contrast to MMC, trabectedin does not induce any significant accumulation of FA cells in G<sub>2</sub>-M. The critical relevance of FA proteins in the response of

human cells to trabectedin reported herein, together with observations showing the role of the FA pathway in cancer suppression, strongly suggest that screening for mutations in FA genes may facilitate the identification of tumors displaying enhanced sensitivity to this novel anticancer drug. [Mol Cancer Ther 2008;7(5):1309–18]

## Introduction

Trabectedin (ET-743; Yondelis; Fig. 1A) is a potent antitumor drug currently undergoing phase II/III clinical trials that has recently received regulatory approval from the European Medicines Agency for the treatment of metastatic or advanced soft-tissue sarcoma after failure to anthracyclines and ifosfamide (1). Trabectedin binds in the DNA minor groove by establishing a covalent bond with the exocyclic 2-amino group of a guanine in one strand and one or two hydrogen bonds with other DNA bases in the opposite strand (Fig. 1B) depending on sequence context (2). This type of interaction differs from that observed for other DNA-binding antitumor drugs and could account for some of the distinctive pharmacologic features of trabectedin, such as the potent and rapid inhibition of activated but not constitutive transcription (3, 4) and the atypical response detected in cells with deficiencies in nucleotide excision repair (NER). In this latter respect, whereas all known DNA-interacting drugs are either more effective or equally effective in NER-deficient cells relative to their NER-proficient counterparts (5–8), trabectedin is paradoxically less cytotoxic in NER-deficient cells (9–12), particularly in those harboring a deleterious mutation in the XPG endonuclease (11, 13). On the other hand, experimental evidence from different laboratories has shown that both yeast mutants with gene deletions in the *RAD52* epistasis group [e.g., *Saccharomyces cerevisiae rad52Δ* (9) and *Schizosaccharomyces pombe rad51Δ* and *rad54Δ* cells (13, 14)] and mammalian cells deficient in *XRCC3*, *BRCA2*, *RAD51C*, and *XRCC2* (15) are much more sensitive to trabectedin than their normal counterparts. Because proteins encoded by these genes are components of the homologous recombination (HR) machinery, which is required for the repair of double-strand breaks (DSBs) associated with replication forks (16), all these data indicate that HR participates in the processing of the DNA lesions induced by trabectedin, including the generation and repair of DSBs (15, 17, 18). Given the unique mode of binding of trabectedin to DNA and the feasibility of having two or more trabectedin molecules simultaneously targeting adjacent or closely spaced sites on opposing strands (19, 20), we reasoned that this type of covalent adduct might functionally mimic an interstrand cross-link (ICL) such as that produced by the potent antitumor and bifunctional cross-linking agent mitomycin

Received 12/27/07; revised 2/21/08; accepted 2/29/08.

**Grant support:** Comisión Interministerial de Ciencia y Tecnología SAF2005-00058 (J.A. Bueren) and SAF2006-12713-C02-02 (F.G.), Comunidad de Madrid S-BIO/0214/2006 (F. Gago), and Marcelino Botín Foundation to promote Translational Research on Biomedicine 2005-2009 (J.A. Bueren).

The costs of publication of this article were defrayed in part by the payment of page charges. This article must therefore be hereby marked *advertisement* in accordance with 18 U.S.C. Section 1734 solely to indicate this fact.

**Requests for reprints:** Juan A. Bueren, Division of Hematopoiesis and Gene Therapy Program, Centro de Investigaciones Energéticas, Medioambientales y Tecnológicas, Avenida Complutense 22, 28040 Madrid, Spain. Phone: 34-91-3466518; Fax: 34-91-3466484. E-mail: juan.bueren@ciemat.es

Copyright © 2008 American Association for Cancer Research.

doi:10.1158/1535-7163.MCT-07-2432

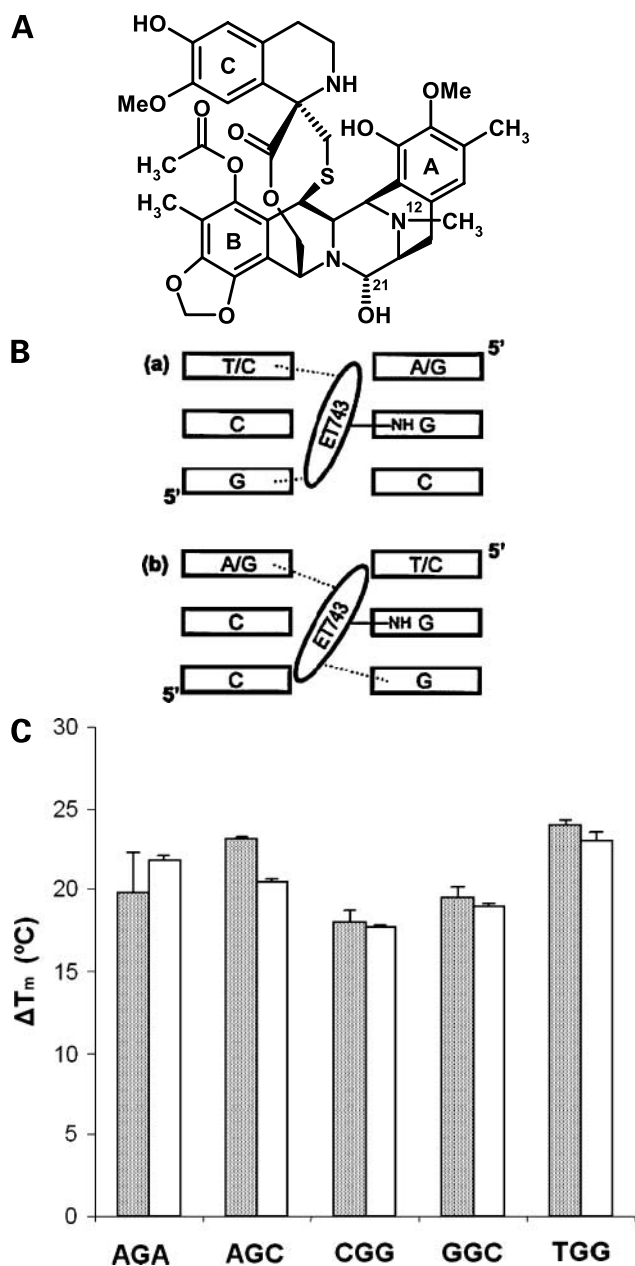


**Figure 1.** Analysis of the trabectedin adducts formed after incubation with selected duplex oligodeoxynucleotides. **A**, chemical structure of trabectedin. **B**, predicted mode of binding of trabectedin (ET-743) to dsDNA. Drug-DNA covalent bonds and hydrogen-bonding interactions are drawn, respectively, as *solid* and *dotted* lines in the two main types of complexes (**a** and **b**). **C**, increases in the melting temperatures of selected duplex oligodeoxynucleotides containing a single trabectedin covalent adduct in their central region following incubation with the drug for either 15 min (*shaded columns*) or 24 h (*open columns*). Mean  $\pm$  SE of three independent experiments.

C (MMC; Supplementary Fig. S1;<sup>6</sup> ref. 21). ICLs represent a major threat to cell viability, insofar as they are highly

effective in blocking replication and transcription forks (5). ICL resolution is known to occur through the coordinated action of multiple DNA repair pathways, including NER and HR, in a process that gives rise to DSBs because both DNA strands are covalently modified and need to be incised (16, 22).

Because of the reported structural characteristics of trabectedin-DNA adducts (2) we decided to investigate the extent to which a single drug molecule is able to stabilize dsDNA using a highly sensitive fluorescence-based melting assay (23). Increases in the thermal stability of the double helix suggested that trabectedin might mimic the cellular effects induced by ICL drugs. In this respect, previous studies have shown that cells deficient in the Fanconi anemia (FA) pathway display high sensitivity and show a characteristic accumulation in the G<sub>2</sub>-M phase of the cell cycle after treatment with ICL drugs (24). Thus far, 13 different FA genes have been cloned, which code for proteins forming part of the upstream FA core complex (FANCA, FANCB, FANCC, FANCE, FANCF, FANCG, FANCL, and FANCM), for proteins of the FA-ID complex (FANCI and FANCD2), or for proteins functioning downstream the FA-ID complex (FANCD1/BRCA2, FANCI/BRIP1, and FANCN/PALB2; see review in ref. 25). Significantly, proteins participating in all of these different steps of the FA pathway have been related to DNA repair and cancer suppression (26–30).

Our data show for the first time that cells with mutations in any of the FA genes tested are extraordinarily sensitive to trabectedin. This finding provides new clues for understanding the mechanism of action of trabectedin in human cells and strongly suggests that tumors incapable of activating the FA pathway will be particularly sensitive to this anticancer drug.

## Materials and Methods

### Fluorescence Melting Experiments

Synthetic oligodeoxynucleotides with one strand 5'-end labeled with the fluorophore 6-carboxyfluorescein (F) and the complementary strand 3'-end labeled with the fluorescence quencher tetramethylrhodamine (Q) were synthesized and purified by high-performance liquid chromatography as a single peak by Bonsai Technologies Group. Annealing of each F-oligonucleotide with its complementary Q-oligonucleotide at a final duplex concentration of 0.1  $\mu$ mol/L in TAE buffer [0.08 mol/L Tris-acetate, 2 mmol/L EDTA (pH 7.5)] was accomplished in a PTC-100 thermocycler (MJ Research) by first heating to 95°C for 5 min and then gradually cooling down to 20°C at a rate of 1°C/min. Correct annealing was confirmed by monitoring the quenching in fluorescence that takes place when F and Q are placed in proximity on formation of a double-stranded structure. The melting reactions were carried out in 96-well plates loaded with the preannealed double-stranded oligonucleotides in a total volume of 20  $\mu$ L TAE buffer at a final concentration of 0.1  $\mu$ mol/L either in the absence or in the presence of the drug. Trabectedin was dissolved in DMSO and serially diluted in the same solvent to yield final concentrations from 0.01 to 0.1  $\mu$ mol/L. The

<sup>6</sup>Supplementary data for this article are available at Molecular Cancer Therapeutics Online (<http://mct.aacrjournals.org/>).

mixtures were incubated for either 15 min or 24 h at 37°C before the melting assay was started in a 7500 Fast Real-Time PCR System (ABI Prism, Applied Biosystems) by increasing the temperature in small steps of 1°C/min up to 95°C. By recording the changes in fluorescence at 517 nm in the FAM channel obtained as a function of the temperature and calculating the midpoint of the transition ( $T_m$ ), we were able to estimate the increases in melting temperatures ( $\Delta T_m$ ) brought about by drug binding. A series of custom-designed oligonucleotides were designed to provide a single occurrence of all possible binding sites for trabectedin in a single central triplet (Supplementary Fig. S2),<sup>6</sup> and all measurements were done in triplicate. The raw data recovered from the instrument for each plate consisted of an array of FAM fluorescence values for each of the 96 wells at each temperature. A complete analysis was then carried out using an in-house Visual Basic Application running on Microsoft Excel (23).

#### Cell Lines

Human fibroblastic cells FA-A (PD220), FA-C (PD331), and FA-G (PD352) were obtained from the Oregon Health Sciences University Fanconi Anemia Cell Repository. FA-D1 fibroblasts (HSC62) were kindly provided by Helmut Hanenberg. The normal diploid human lung fibroblast-like cell line, MRC-5, was kindly provided by J. Surrallés. Fibroblastic human cell lines derived from healthy donors and FA patients were cultured in DMEM supplemented with 10% fetal bovine serum (Lonza), 2 mmol/L L-glutamine (Life Technologies), 100 units/mL penicillin, and 100 µg/mL streptomycin (Pen-Strep, Life Technologies) and kept at 37°C in a humidified atmosphere with 5% CO<sub>2</sub>. EBV-transformed lymphoblast cell lines (LCLs) were generated from healthy donors and from FA-A (FA88; ref. 31), FA-C (HSC526), and FA-F (EUFA698) patients. FA-C and FA-F LCLs were kindly provided by Helmut Hanenberg. LCLs were maintained in RPMI (Life Technologies) supplemented with 20% fetal bovine serum (Life Technologies) and antibiotics.

#### Analysis of the Cellular Sensitivity to Trabectedin, MMC, and Ethylnitrosourea

For assessing the sensitivity of fibroblast cell lines to the drugs, aliquots of 10,000 cells per well were seeded in 96-well plates (BD Falcon) in subconfluent conditions. On the next day, fresh medium containing increasing concentrations of the drugs was added. Twenty-four hours later, the culture medium was removed and replaced with fresh medium without the drugs. Three days after, the cell viability was tested using the 3-(4,5-dimethyl-2-thiazolyl)-2,5-diphenyltetrazolium bromide assay, which is based on the protocol described by Mossmann (32). Briefly, cells were incubated for 3 h with 0.45 mg/mL 3-(4,5-dimethyl-2-thiazolyl)-2,5-diphenyltetrazolium bromide (Sigma), dissolved previously in serum-free medium. Cultures were washed with PBS followed by the addition of DMSO (Sigma), and gentle agitation for the complete dissolution of the insoluble purple formazan product into a colored solution. The absorbance of this colored solution was quantified by measuring in a microplate reader

(GeniosPro, Tecan). Cell viability was expressed as the percentage of the absorbance value determined in wells in which there was no drug (considered as 100% of viability). Analyses of the viability of LCLs were determined essentially as described previously (31). Five days after treatment with the drugs, cells were resuspended in PBS-bovine serum albumin (BSA; 0.05%) containing 0.5 µg/mL propidium iodide (Sigma) and incubated for 10 min at 4°C. Cell viability was determined by flow cytometry (EPICS, Coulter Electronics) based on the propidium iodide exclusion test using a dot blot of forward scatter versus propidium iodide fluorescence. MMC (Life Technologies) and trabectedin (PharmaMar) were kept at -80°C as 1 mmol/L stock solutions and ethylnitrosourea (Sigma) as a 0.1 mol/L stock solution.

#### Cytometric Analysis of $\gamma$ H2AX as a Surrogate Marker of DNA DSBs

Histone H2AX phosphorylated on Ser<sup>139</sup> ( $\gamma$ H2AX) was quantitated by flow cytometry as reported previously (33). Aliquots of 10<sup>5</sup> cells were washed in PBS and fixed in suspension in 4.5 mL ice-cold 1% methanol-free formaldehyde in PBS for 15 min on ice. After centrifugation, cells were resuspended in 5 mL of 70% ethanol (0-4°C) and stored at -20°C at least for 2 h. Cells were washed twice in PBS, centrifuged, and blocked with 1 mL of 1% BSA and 0.2% Triton X-100 in PBS (BSA-T-PBS) for 30 min at room temperature. After centrifugation cells were incubated in BSA-T-PBS containing 1 µg  $\gamma$ H2AX antibody (Upstate Biotechnology) overnight at 4°C. Cells were washed twice in BSA-T-PBS and incubated in BSA-T-PBS with Alexa Fluor 488-conjugated F(ab)<sub>2</sub> fragment of goat anti-mouse secondary antibody (1:100 dilution; Molecular Probes) for 1 h at room temperature with gentle shaking. After washing, cells were resuspended in 1 mL propidium iodide solution 5 µg/mL (Molecular Probes) and 100 µg/mL DNase-free RNase A (Sigma) and incubated for 30 min at 37°C. Finally, cells were analyzed by flow cytometry (Coulter XL) with bivariate dot-plot analysis of  $\gamma$ H2AX fluorescence and linear fluorescence of propidium iodide (DNA content) from 10,000 events with doublet discrimination. Analyses of cell cycle phases were done using the MODFIT LT software (Verity Software House). The background percentage of  $\gamma$ H2AX in untreated cells was set between 3% and 7%. Increases over background values were determined in each experimental group.

#### Immunofluorescence Studies of $\gamma$ H2AX and RAD51 Foci Formation

Cells were seeded in cover slides treated previously with 2 µg/cm<sup>2</sup> retronectin (Takara Shuzo). After treatment with MMC or trabectedin, cells were washed and fixed with 3.7% paraformaldehyde in PBS. Fixation was followed by permeabilization with 0.5% Triton X-100 in PBS for 5 min. After 30 min in blocking buffer (10% fetal bovine serum, 0.1% NP-40 in PBS), cells were incubated overnight with either anti-RAD51 rabbit antibody (PC130; 1:200 dilution; Calbiochem) and/or anti- $\gamma$ H2AX mouse antibody (1:2,000 dilution). Cells were then washed three times in TBS and subsequently incubated with secondary antibodies: Texas

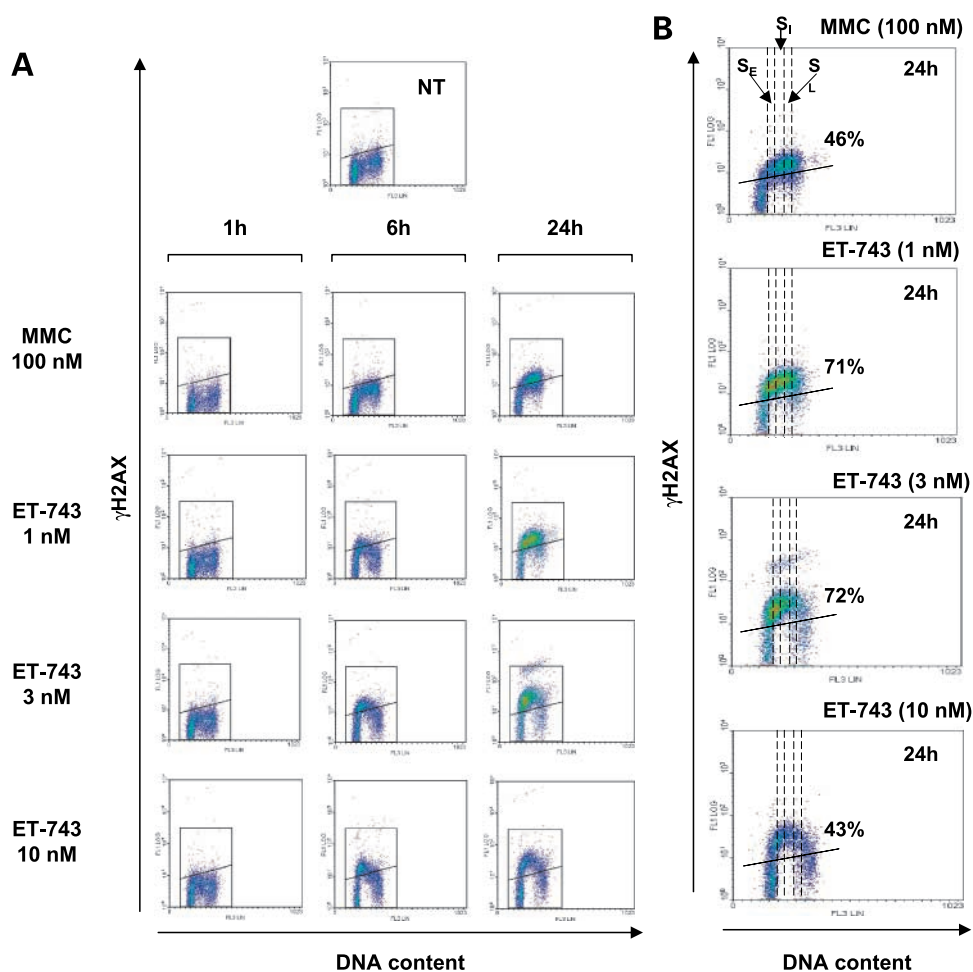


**Figure 2.** Generation of DNA DSBs in human MRC-5 fibroblasts treated with either MMC or trabectedin. **A**, representative flow cytometry analysis of  $\gamma$ H2AX in MRC-5 cells treated with MMC and trabectedin (ET-743). **B**, detailed analysis of the generation of  $\gamma$ H2AX in cells treated for 24 h with MMC or trabectedin (ET-743). SE, SI, SL; early, intermediate, and late S phase, respectively.

Red-conjugated anti-rabbit polyclonal antibody (Jackson ImmunoResearch Laboratories) to detect RAD51 foci and Alexa Fluor 488 nm anti-mouse monoclonal antibody (Molecular Probes) for  $\gamma$ H2AX detection. After 45 min, cells were washed for three times with TBS and slides were mounted in Moviol with 4,6-diamidino-2-phenylindole. Two hundred cells were scored using a fluorescence microscope (Zeiss Axioplan2), and cells with >10 foci of each marker protein were scored as positive (31).

#### Statistical Methods

Results from 3-(4,5-dimethyl-2-thiazolyl)-2,5-diphenyltetrazolium bromide assays were calculated as survival percentages respect to control cultures exposed to DMSO 0.1% (final concentration of drug vehicle in cultures). In Figs. 4 and 5, statistical differences between means were evaluated by using Student's *t* test. Differences were considered significant when  $P \leq 0.05$ . Results are reported as mean  $\pm$  SE of at least three independent experiments.

## Results

### A Single Trabectedin Adduct Greatly Stabilizes dsDNA

The thermal stability of different duplex oligodeoxynucleotides, each containing a unique binding site for

trabectedin in the central region, was assessed by means of a previously reported method based on molecular beacons (23). These duplexes encompass the two-hydrogen-bond-compliant purine-G-C and pyrimidine-G-G combinations shown in Fig. 1B as well as the more recently characterized AGA triplet for which only one hydrogen bond is possible (34, 35). The consistently high increment in melting temperature of dsDNA (average  $\Delta T_m \geq 20^\circ\text{C}$ ) was at least 2-fold greater than that brought about by a tight-binding bisintercalating agent such as echinomycin or thiocoraline (23) and was essentially identical after 15 min or 24 h of incubation in the whole range of drug/DNA ratios studied (1:10 to 1:1). The extra DNA stabilization was very similar for all the duplexes that embedded one of the preferred binding sequences in the central triplet irrespective of the number of hydrogen bonds (Fig. 1C), whereas the disfavored sequence studied, CGA (34, 35), was not stabilized at all (data not shown). These results are consistent with previous findings using plasmid DNA molecules (35, 36) and argues strongly in favor of the view that the hampering of DNA strand separation brought about by the covalent adduct may result in a strong blockade of transcription and replication forks in living cells. This behavior is reminiscent of that elicited by

other antineoplastic drugs that give rise to true ICLs such as MMC (37).

#### Therapeutic Doses of Trabectedin Induce DNA DSBs and Activate HR Repair in Human Cells

Because a single trabectedin adduct was very effective in hampering DNA strand separation, we asked whether low concentrations of trabectedin, similar to those observed in the plasma of patients treated with this drug (38), could result in the generation of DSBs in the DNA of cultured cells.

As deduced from the analysis of the  $\gamma$ H2AX, treatment of MRC5 fibroblasts with either trabectedin or MMC induced DSBs (Fig. 2). Of note, doses of trabectedin as low as 3 nmol/L and even 1 nmol/L were sufficient to generate DSBs. Nonetheless, whereas MMC induced a predominant  $\gamma$ H2AX marking in the intermediate/late S phase of the cell cycle, in trabectedin-treated cells, a high proportion of  $\gamma$ H2AX staining could be observed in the early stages of the S phase (see representative analyses in Fig. 2B). Interestingly, the percentages of  $\gamma$ H2AX-positive cells after 24-h exposures were lower in cells treated with 10 nmol/L trabectedin than in cells exposed to the lower concentrations of 1 or 3 nmol/L trabectedin (43% versus 71% and 72%, respectively).

The generation of DSBs in human cells treated with low doses of trabectedin was confirmed in human

LCLs (see representative analyses in Fig. 3A). Moreover, kinetic analyses of  $\gamma$ H2AX marking in these cells confirmed the higher efficacy of low (3 nmol/L) versus higher (10 nmol/L) doses of trabectedin to generate DSBs in these cells (Fig. 3B). Because differences in the generation of DSBs by 1 to 10 nmol/L trabectedin could be related to differences in the cell cycle status of the cells, we also determined the kinetics of  $\gamma$ H2AX marking within the S phase of trabectedin-treated cells (Fig. 3B). Once again, these analyses confirmed the very high efficacy of trabectedin for generating DSBs within the S phase (90% of LCLs in S phase were positive for  $\gamma$ H2AX after a 72-h exposure to 1 nmol/L of the drug) and showed that the relatively high dose of 10 nmol/L gives rise to a plateau effect when cells are exposed to the drug for 6 to 72 h.

Because HR constitutes an error-free repair mechanism that can participate in the processing of DNA ICLs and DSBs, we investigated whether therapeutic doses of trabectedin could activate the HR machinery of the cell. To this aim, the generation of nuclear RAD51 foci was determined immediately after and 40 h after a 6-h treatment with trabectedin (Fig. 4). As was the case in MMC-treated cells, a significant increase in the proportion of RAD51-positive cells was observed immediately after the 6-h exposure with trabectedin, an effect that persisted at least 40 h later. As shown in the representative pictures

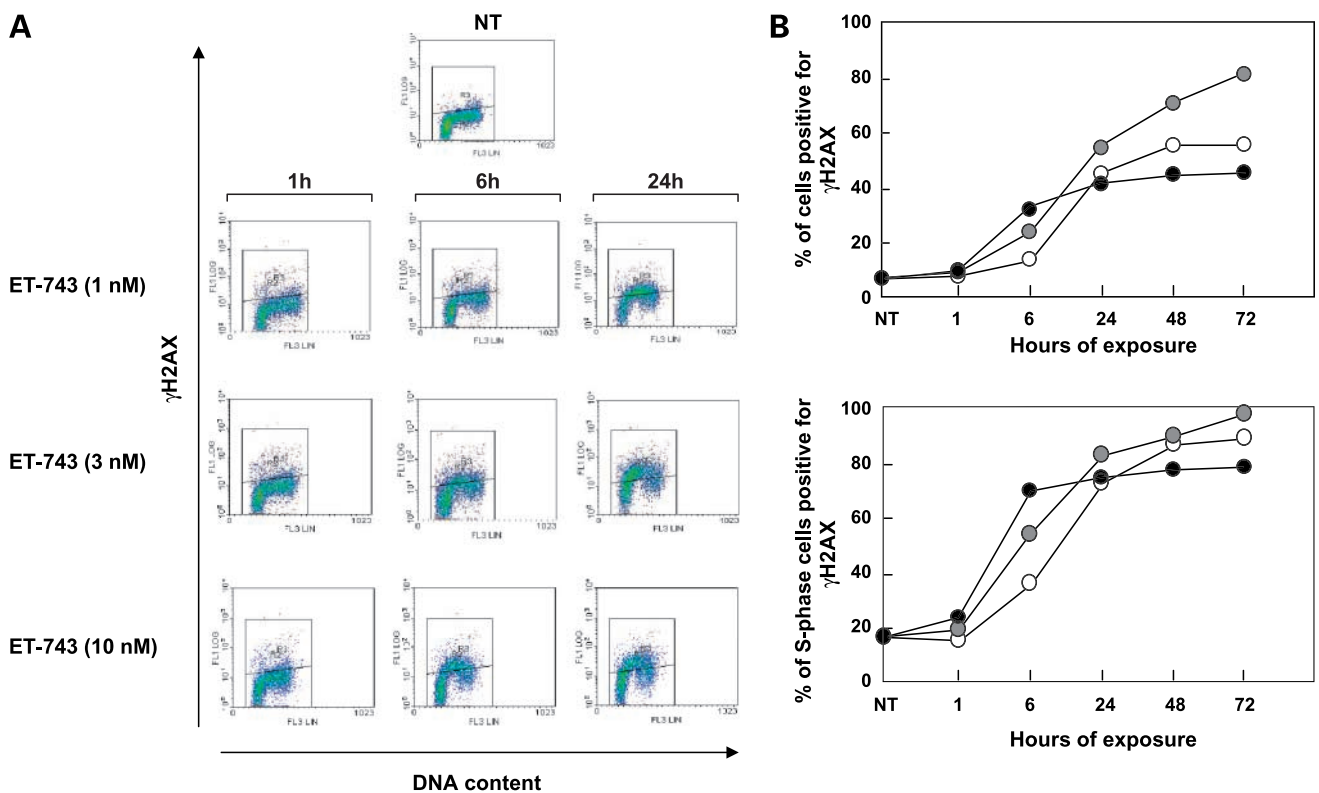


**Figure 3.** Generation of DNA DSBs in human LCLs treated with trabectedin. **A**, representative analyses of  $\gamma$ H2AX in human LCLs treated with trabectedin (ET-743) for 1, 6, and 24 h. **B**, time course analysis of  $\gamma$ H2AX in human LCLs treated with 1 nmol/L (○), 3 nmol/L (◐), or 10 nmol/L (●) trabectedin for 1 to 72 h. *Bottom*, proportion of cells in S phase that were positive for  $\gamma$ H2AX staining. Representative experiment.

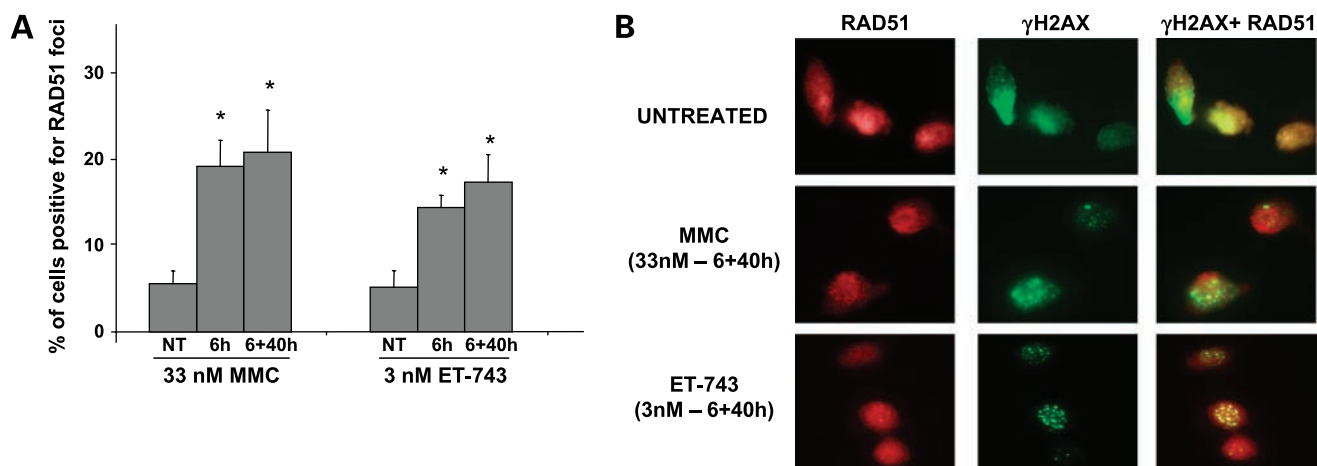


**Figure 4.** Induction of nuclear Rad51 foci in human LCLs treated with MMC and trabectedin (ET-743). **A**, proportion of RAD51-positive cells in untreated cells (NT) and in cells exposed for 6 h to MMC (33 nmol/L) or trabectedin (ET-743; 3 nmol/L) and analyzed immediately after treatment (6 h) or 40 h later (6 + 40 h). **B**, representative pictures showing RAD51-foci and  $\gamma$ H2AX-foci in LCLs treated with MMC and trabectedin. Original magnification,  $\times 1,000$ . Mean  $\pm$  SE of three independent experiments. \*,  $P < 0.05$ , significant differences between the proportion of cells positive for RAD51 foci in samples not exposed to the drugs and samples exposed to MMC or ET-743.

of Fig. 4, RAD51 always colocalized with  $\gamma$ H2AX, in good consistency with the notion that RAD51 is recruited at sites of DSBs to facilitate their repair via HR.

#### Disruption of the FA Pathway Hypersensitizes Human Cells to Trabectedin

To study in more detail whether trabectedin mimicked the action of classic ICL drugs, we investigated whether one of the characteristic effects of these drugs, in particular their exacerbated cytotoxicity on cells deficient in the FA pathway, was also applicable to trabectedin. To this end, the effect of trabectedin on human fibroblasts competent in the FA pathway (MRC-5 cells) was compared with that on FA-A, FA-C, and FA-G fibroblasts (deficient in proteins of the FA core complex: FANCA, FANCC, and FANCG) and also on FA-D1 fibroblasts (deficient in FANCD1/BRCA2, a downstream protein in the FA pathway). MMC and ethylnitrosourea were used as positive and negative controls because ethylnitrosourea can only form mono-adducts in a single DNA strand. As expected, all the FA fibroblasts tested were hypersensitive to MMC. Interestingly, fibroblasts deficient in proteins of the FA core (FA-A, FA-C, and FA-G cells) as well as FA-D1 fibroblasts were much more sensitive to trabectedin than wild-type (WT) cells ( $IC_{50}$  values were on average 8-fold lower; Fig. 5). In contrast to this observation, FA cells were not hypersensitive to ethylnitrosourea (Fig. 5). To confirm these findings, the sensitivity to trabectedin of FA-A, FA-C, and FA-F LCLs was also tested. Once again, FA cells (in these case, human FA LCLs) were highly sensitive to trabectedin compared with LCLs from healthy donors ( $IC_{50}$  values were 10-fold lower; Fig. 5). Taken together, these results show a similar dependence on the FA pathway to process the DNA damage induced by trabectedin and the classic ICL drug MMC but not by the agent that gives rise exclusively to monoadducts. The fact that mutations in genes encoding for

proteins of the FA core complex (FANCA, FANCC, FANCF, and FANCG) as well as in the FANCD1/BRCA2 gene confer cell hypersensitivity to trabectedin unequivocally establishes the critical relevance of the FA/BRCA pathway in the repair of the DNA damage induced by this drug.

#### Comparative Cell Cycle Analysis in Cells Treated with Trabectedin or MMC

To further investigate the cellular effects induced by trabectedin in comparison with those evoked by classic ICL drugs, we determined the cell cycle kinetics of WT and FA LCLs treated with trabectedin or MMC (Fig. 6). In WT cells, short exposures of 1 h with either drug induced an accumulation of cells in the S phase. On the other hand, prolonged exposures (48–72 h) to MMC induced cell accumulations in  $G_1$ , whereas the same exposures to 1, 3, and 10 nmol/L trabectedin induced cell accumulations in  $G_2$ -M, S, and  $G_1$ -S, respectively.

The cell cycle differences observed in cells treated with either MMC or trabectedin were even more striking when FA cells were used. Although the expected accumulation of FA-A cells in  $G_2$ -M was observed after MMC treatment (24–72 h exposures), none of the tested doses of trabectedin was capable of inducing any significant accumulation in  $G_2$ -M of FA-A cells, which were instead blocked in  $G_1$  (see representative analyses in Fig. 6).

To investigate whether this striking difference between MMC and trabectedin was exclusively produced in FA-A cells, similar experiments were conducted in FA-C cells subjected to either acute (6 h) or chronic (up to 72 h) exposures to the drug. Data in Supplementary Fig. S3<sup>6</sup> confirmed the previously observed differences in the cell cycle response evoked by both drugs in FA cells. As happened in FA-A cells (see Fig. 6), chronic or acute exposures to trabectedin did not induce accumulation of FA-C cells in  $G_2$ -M (Supplementary Fig. S3<sup>6</sup>).

This final set of experiments clearly shows that the FA pathway is playing different roles in cell cycle control in the cells treated with either MMC or trabectedin. Thus, although our previous data in this study suggested that trabectedin mimics many of the DNA and cellular effects induced by classic ICL drugs, the characteristic blockade of FA cells in G<sub>2</sub>-M elicited by the representative drug MMC is not reproduced by trabectedin.

## Discussion

Although previous studies have investigated the mechanism(s) by which trabectedin inhibits cell growth (3, 9–13, 35, 36), the primary mechanism accounting for the potent antiproliferative effects of trabectedin in some cancer cell types is still poorly understood. A cancer cell line selected *in vitro* for its enhanced resistance to trabectedin (11) lacked a functional XPG (ERCC5), the structure-specific DNA endonuclease that makes the first 3' incision on ssDNA during NER and transcription-coupled NER (39). Similarly, *S. pombe* cells deficient in *rad13* (the yeast orthologue of XPG) also displayed increased resistance to trabectedin and underwent much less DNA damage than the corresponding isogenic WT strain. However, additional experiments showed that it is not the missing endonuclease activity of this protein that confers resistance to trabectedin but the lack of a highly conserved basic residue in the DNA-binding domain that can presumably stabilize a *rad13*/DNA/trabectedin ternary complex through a direct interaction with the drug (13). This rather unique mechanism can account for the unusual behavior of these mutant cells because defects in NER proteins, which are involved in the repair of DNA damage caused by many DNA-binding anticancer drugs (e.g., the nitrogen mustard mechlorethamine, cisplatin, or MMC; refs. 5, 6), typically lead to increased drug sensitivity (5, 40, 41) and not the reverse, as is the case for trabectedin.

In contrast to observations made in NER-deficient cells, experiments on yeast and mammalian cells harboring

specific deletions in HR genes (e.g. *RAD51C*, *XRCC2*, *XRCC3*, and *BRCA2*) have shown that HR mutants are highly sensitive to trabectedin (9, 13, 15). Because loss of HR repair was associated with the persistence of unrepaired DSBs, it has been proposed that DSBs play a key step in the processing of the DNA lesions produced by this drug (15). Furthermore, a strict requirement for DNA synthesis in the formation of these DSBs has been recently shown (15).

Based on these observations, and because of the particular structure of trabectedin, which endows it with the ability to form a covalent adduct with one DNA strand and simultaneously establish at least one hydrogen bond and extensive hydrophobic contacts with the complementary strand (Fig. 1B; refs. 2, 19, 20), we first investigated the extent to which trabectedin is able to stabilize dsDNA using a highly sensitive and accurate fluorescence-based method. Noteworthy, our analyses of the thermal stability of different duplex oligodeoxynucleotides each containing a single tailor-made trabectedin-DNA adduct showed a marked stabilization of the double helix following incubation with trabectedin (Fig. 1C). These results are compatible with the idea that DNA strand separation will be hampered intracellularly in the presence of the bonded drug, with the covalent adduct(s) behaving in practice similarly to an ICL, as reported for agents such as cisplatin (42) and the nitrogen mustard mechlorethamine (in a low percentage of lesions; ref. 43) or MMC (under reducing conditions; ref. 21). This hypothesis raised the interesting possibility that removal of the trabectedin-DNA adducts might require the same repair machinery that cells use for removing ICLs.

Although recent data have shown the generation of  $\gamma$ H2AX foci after treatment with high doses of trabectedin (10–100 nmol/L; ref. 15), we were interested in understanding whether clinically relevant doses of trabectedin (~1–3 nmol/L; ref. 38) were also capable of inducing DSBs in human DNA compared with MMC.

Our  $\gamma$ H2AX analyses showed that trabectedin recapitulates the DSBs induced by MMC in human cells even

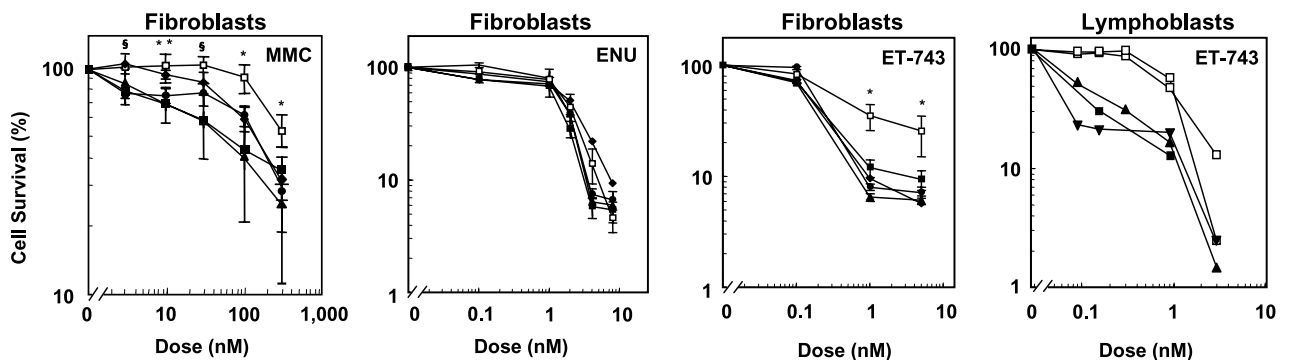


**Figure 5.** Increased sensitivity of human cells deficient in the FA/BRCA pathway to MMC and trabectedin (ET-743) but not to ethylnitrosourea (ENU). WT and FA fibroblastic and LCLs were treated with the drugs and analyzed for viability as indicated in Materials and Methods. Survival curves corresponding to WT (□), FA-A (▲), FA-C (■), FA-F (▼), FA-G (●), and FA-D1 (◆) are shown. Mean  $\pm$  SE of three to five independent experiments. \*,  $P < 0.05$ , significant differences between the control group and all groups of FA cells; §, significant differences between the control group and FA-A and FA-C cells; \*\*, significant differences between the control group and FA-A, FA-C, and FA-G cells.

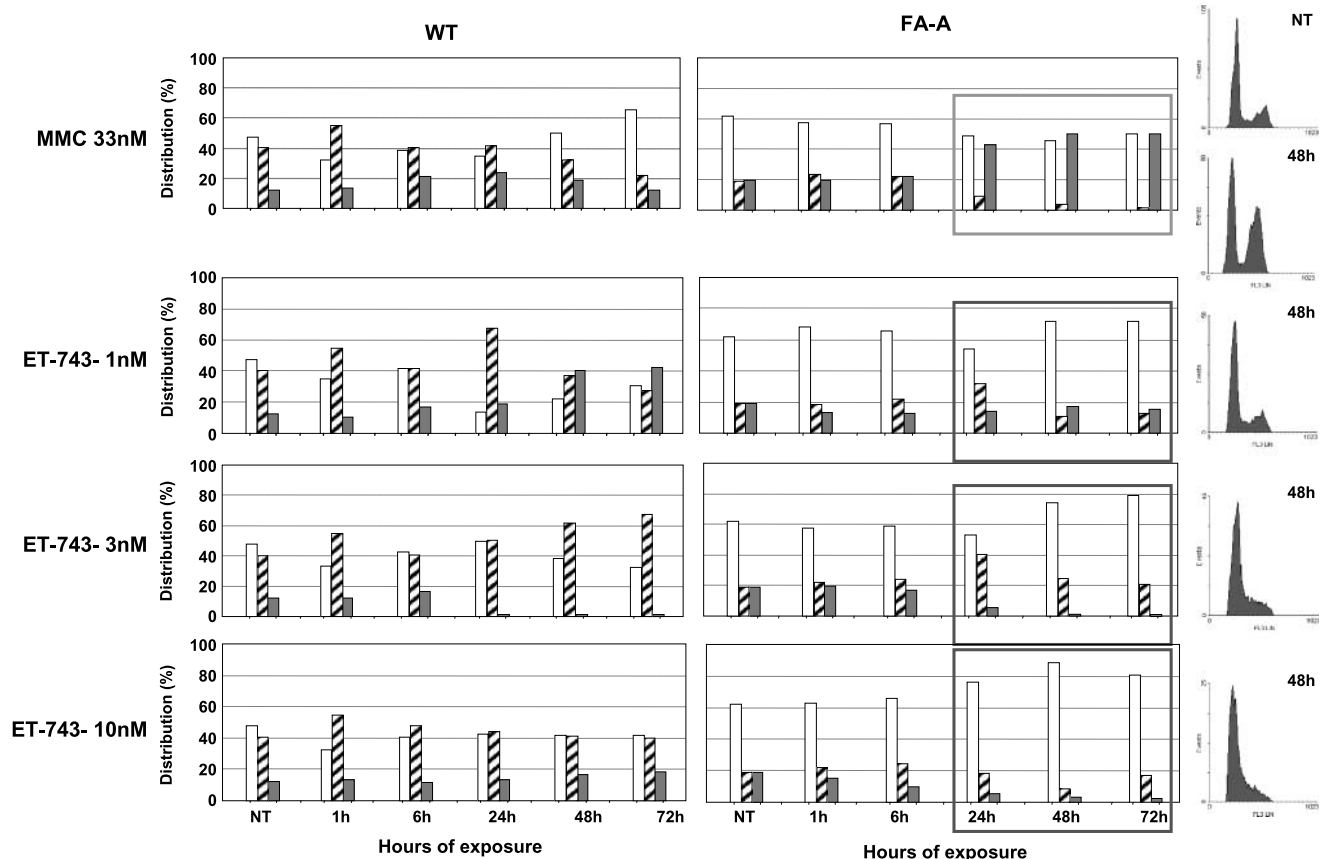


**Figure 6.** Cell cycle analysis of WT and FA-A human LCLs treated with either MMC or trabectedin. Cell cycle distribution of WT and FA-A LCLs exposed to 33 nmol/L MMC or to 1, 3, or 10 nmol/L trabectedin (ET-743) for 1 to 72 h. *Open columns*, G<sub>1</sub>; *striped columns*, S; *gray columns*, G<sub>2</sub>-M. Right panels show representative cell cycle histograms of FA-A cells either untreated (NT) or treated with MMC or ET-743 for 48 h (48 h).

when used at concentrations as low as 1 nmol/L (expected to be attained in the tumor cells of patients enrolled in the clinical studies; ref. 38). In good consistency with data reported for other cell types at a variety of concentrations (15), we observed the specific generation of DSBs during the S phase of the cell cycle (Fig. 3). Nonetheless, it is worth pointing out that our studies consistently show the relative inefficacy of 10 nmol/L trabectedin for inducing DSBs in human cells, compared with the lower, clinically relevant concentrations of 1 and 3 nmol/L, provided that sufficiently long incubation times (24-72 h) are allowed (Fig. 3B). Because the cytotoxic effects of trabectedin are clearly dose dependent (Fig. 5), the above-mentioned observation possibly points to some differences in the cytotoxic mechanism(s) at low and high concentrations of trabectedin. In fact, previous evidence has suggested two distinct and dose-dependent signaling routes that can be activated as a consequence of trabectedin treatment: a transcription-dependent pathway leading to cell cycle arrest and a transcription-independent pathway leading to rapid apoptosis (44).

As reported previously for MMC-treated cells (see Fig. 4A and data in ref. 45), trabectedin also promoted the

translocation of RAD51 to the nucleus of cells in which DSBs had been generated, most likely as structural intermediates required for the correct processing of the trabectedin-DNA adducts (15). The observation that RAD51 was codetected with  $\gamma$ H2AX in the same nuclear foci (Fig. 4B) is consistent with the idea that it is the DSB itself rather than the trabectedin-DNA adduct that induces the translocation of RAD51 to the site of the DNA damage to facilitate DNA repair via HR.

Based on the similarities in the generation of DSBs and activation of the HR machinery between trabectedin and MMC, we investigated whether the characteristic hypersensitivity of FA cells to ICL drugs was reproduced when FA cells were treated with trabectedin. In good consistency with recently published data (15), we observed that FA-D1 cells (lacking a functional BRCA2 protein that participates downstream the FANCI/FANCD2 complex; ref. 46) are hypersensitive to both trabectedin and MMC. Moreover, our data show for the first time that FA cells deficient in proteins of the FA core (upstream the FANCI/FANCD2 complex; FANCA, FANCC, FANCF, and FANCG; ref. 47) are also hypersensitive to trabectedin (Fig. 5).



Data showing that cells deficient in FA/BRCA2 proteins are hypersensitive to both MMC and trabectedin not only provide a link between the FA pathway and the response of human cells to trabectedin but also disclose a hitherto unknown similarity in the mechanism of action of these two minor groove binding drugs.

Although trabectedin mimicked the action of MMC with respect to both generation of DSBs and participation of the FA pathway in the processing of the DNA damage, marked differences were noted in the effects of these two drugs on the cell cycle of WT cells, which were even more accentuated in FA cells. Thus, in contrast to the accumulation of FA cells in G<sub>2</sub>-M after treatment with DNA ICL agents (48), our data in Fig. 6 and Supplementary Fig. S3<sup>6</sup> clearly show that trabectedin does not induce any significant blockade of FA-A and FA-C cells in G<sub>2</sub>-M. The rationale for the mechanisms underlying these differential effects on cell cycle progression is currently unclear. Nevertheless, differences in the nature of the interaction of these drugs with the DNA, in the mechanism of checkpoint activation, or in the disruption of other cellular functions such as gene transcription may account for these discrepancies.

Finally, the mounting evidence showing that mutations in genes coding for proteins that participate in the FA pathway have a role in cancer (26–30) underscores the relevance of screening for mutations in FA genes in cancer cells from treatment-eligible patients because tumors with a disrupted FA pathway are likely to display enhanced sensitivity to trabectedin.

## Disclosure of Potential Conflicts of Interest

L. Perez and J.C. Tercero: PharmaMar employees. J.A. Casado, P. Rio, E. Marco, B. Albella, F. Gago, and J.H. Bueren: PharmaMar grant support. The other authors reported no potential conflicts of interest.

## Acknowledgments

We thank Sergio García for invaluable help in the experimental work.

## References

- Schoffski P, Wolter P, Clement P, et al. Trabectedin (ET-743): evaluation of its use in advanced soft-tissue sarcoma. *Future Oncol* 2007;3:381–92.
- Gago F, Hurley LH. Devising a structural basis for the potent cytotoxic effects of ecteinascidin 743. In: Demeunynck M, Bailly C, Wilson WD, editors. *Small molecule DNA and RNA binders: from synthesis to nucleic acid complexes*. Weinheim (Germany): Wiley-VCH; 2002. p. 643–75.
- Friedman D, Hu Z, Kolb EA, Gorfajn B, Scotto KW. Ecteinascidin-743 inhibits activated but not constitutive transcription. *Cancer Res* 2002;62:3377–81.
- Minuzzo M, Marchini S, Brogginini M, Faircloth G, D'Incalci M, Mantovani R. Interference of transcriptional activation by the antineoplastic drug ecteinascidin-743. *Proc Natl Acad Sci U S A* 2000;97:6780–4.
- De Silva IU, McHugh PJ, Clingen PH, Hartley JA. Defining the roles of nucleotide excision repair and recombination in the repair of DNA interstrand cross-links in mammalian cells. *Mol Cell Biol* 2000;20:7980–90.
- Beljanski V, Marzilli LG, Doetsch PW. DNA damage-processing pathways involved in the eukaryotic cellular response to anticancer DNA cross-linking drugs. *Mol Pharmacol* 2004;65:1496–506.
- Koeppel F, Poindessous V, Lazar V, Raymond E, Sarasin A, Larsen AK. Irifolven cytotoxicity depends on transcription-coupled nucleotide excision repair and is correlated with XPG expression in solid tumor cells. *Clin Cancer Res* 2004;10:5604–13.
- Lee YJ, Park SJ, Ciccone SL, Kim CR, Lee SH. An *in vivo* analysis of MMC-induced DNA damage and its repair. *Carcinogenesis* 2006;27:446–53.
- Damia G, Silvestri S, Carrassa L, et al. Unique pattern of ET-743 activity in different cellular systems with defined deficiencies in DNA-repair pathways. *Int J Cancer* 2001;92:583–8.
- Erba E, Bergamaschi D, Bassano L, et al. Ecteinascidin-743 (ET-743), a natural marine compound, with a unique mechanism of action. *Eur J Cancer* 2001;37:97–105.
- Takebayashi Y, Pourquier P, Zimonjic DB, et al. Antiproliferative activity of ecteinascidin 743 is dependent upon transcription-coupled nucleotide-excision repair. *Nat Med* 2001;7:961–6.
- Soares DG, Poletto NP, Bonatto D, Salvador M, Schwartzmann G, Henriques JA. Low cytotoxicity of ecteinascidin 743 in yeast lacking the major endonucleolytic enzymes of base and nucleotide excision repair pathways. *Biochem Pharmacol* 2005;70:59–69.
- Herrero AB, Martin-Castellanos C, Marco E, Gago F, Moreno S. Cross-talk between nucleotide excision and homologous recombination DNA repair pathways in the mechanism of action of antitumor trabectedin. *Cancer Res* 2006;66:8155–62.
- West SC. Molecular views of recombination proteins and their control. *Nat Rev Mol Cell Biol* 2003;4:435–45.
- Soares DG, Escargueil AE, Poindessous V, et al. Replication and homologous recombination repair regulate DNA double-strand break formation by the antitumor alkylator ecteinascidin 743. *Proc Natl Acad Sci U S A* 2007;104:13062–7.
- Arnaudeau C, Lundin C, Helleday T. DNA double-strand breaks associated with replication forks are predominantly repaired by homologous recombination involving an exchange mechanism in mammalian cells. *J Mol Biol* 2001;307:1235–45.
- Guirouilh-Barbat J, Sedelnikova OA, Bonner WM, Pommier Y. Ecteinascidin-induced DNA double strand breaks: a link between histone  $\gamma$ -H2AX, transcription-coupled nucleotide excision repair and Mre11 endonuclease. *AACR Annual Meeting, Washington, DC, 2006*; poster 4642.
- Casado JA, Albella B, Río P, et al. Generation of DNA double-strand breaks during trabectedin (Yondelis) DNA damage measured through induction of  $\gamma$ H2AX. *AACR Annual Meeting, Los Angeles, CA, 2007*; poster 1965.
- Marco E, Garcia-Nieto R, Mendieta J, Manzanares I, Cuevas C, Gago F. A 3.(ET743)-DNA complex that both resembles an RNA-DNA hybrid and mimics zinc finger-induced DNA structural distortions. *J Med Chem* 2002;45:871–80.
- Marco E, Gago F. DNA structural similarity in the 2:1 complexes of the antitumor drugs trabectedin (Yondelis) and chromomycin A3 with an oligonucleotide sequence containing two adjacent TGG binding sites on opposing strands. *Mol Pharmacol* 2005;68:1559–67.
- Iyer VN, Szybalski W. A molecular mechanism of mitomycin action: linking of complementary DNA strands. *Proc Natl Acad Sci U S A* 1963;50:355–62.
- Niedernhofer LJ, Odijk H, Budzowska M, et al. The structure-specific endonuclease Ercc1-Xpf is required to resolve DNA interstrand cross-link-induced double-strand breaks. *Mol Cell Biol* 2004;24:5776–87.
- Negri A, Marco E, Garcia-Hernandez V, et al. Antitumor activity, X-ray crystal structure, and DNA binding properties of thiocoraline A, a natural bisintercalating thiodipeptide. *J Med Chem* 2007;50:3322–33.
- Andreassen PR, Ho GP, D'Andrea AD. DNA damage responses and their many interactions with the replication fork. *Carcinogenesis* 2006;27:883–92.
- Taniguchi T, D'Andrea AD. The molecular pathogenesis of Fanconi anemia: recent progress. *Blood* 2006;107:4223–33.
- Taniguchi T, Tischkowitz M, Ameziane N, et al. Disruption of the Fanconi anemia-BRCA pathway in cisplatin-sensitive ovarian tumors. *Nat Med* 2003;9:568–74.
- Narayan G, Arias-Pulido H, Nandula SV, et al. Promoter hypermethylation of FANCF: disruption of Fanconi anemia-BRCA pathway in cervical cancer. *Cancer Res* 2004;64:2994–7.
- van der Heijden MS, Brody JR, Gallmeier E, et al. Functional defects in the Fanconi anemia pathway in pancreatic cancer cells. *Am J Pathol* 2004;165:651–7.

29. van der Heijden MS, Brody JR, Dezentje DA, et al. *In vivo* therapeutic responses contingent on Fanconi anemia/BRCA2 status of the tumor. *Clin Cancer Res* 2005;11:7508–15.
30. Thompson E, Dragovic RL, Stephenson SA, Eccles DM, Campbell IG, Dobrovic A. A novel duplication polymorphism in the FANCA promoter and its association with breast and ovarian cancer. *BMC Cancer* 2005;5:43.
31. Casado JA, Callen E, Jacome A, et al. A comprehensive strategy for the subtyping of Fanconi anemia patients: conclusions from the Spanish Fanconi Anemia research network. *J Med Genet* 2007;44:241–9.
32. Mosmann T. Rapid colorimetric assay for cellular growth and survival: application to proliferation and cytotoxicity assays. *J Immunol Methods* 1983;65:55–63.
33. Huang X, Darzynkiewicz Z. Cytometric assessment of histone H2AX phosphorylation: a reporter of DNA damage. *Methods Mol Biol* 2006;314:73–80.
34. Marco E, David-Cordonnier MH, Bailly C, Cuevas C, Gago F. Further insight into the DNA recognition mechanism of trabectedin from the differential affinity of its demethylated analogue ecteinascidin ET729 for the triplet DNA binding site CGA. *J Med Chem* 2006;49:6925–9.
35. David-Cordonnier MH, Gajate C, Olmea O, et al. DNA and non-DNA targets in the mechanism of action of the antitumor drug trabectedin. *Chem Biol* 2005;12:1201–10.
36. Zewail-Foote M, Li VS, Kohn H, Bearss D, Guzman M, Hurley LH. The inefficiency of incisions of ecteinascidin 743-DNA adducts by the UvrABC nuclease and the unique structural feature of the DNA adducts can be used to explain the repair-dependent toxicities of this antitumor agent. *Chem Biol* 2001;8:1033–49.
37. Tomasz M, Palom Y. The mitomycin bioreductive antitumor agents: cross-linking and alkylation of DNA as the molecular basis of their activity. *Pharmacol Ther* 1997;76:73–87.
38. Ryan DP, Supko JG, Eder JP, et al. Phase I and pharmacokinetic study of ecteinascidin 743 administered as a 72-hour continuous intravenous infusion in patients with solid malignancies. *Clin Cancer Res* 2001;7:231–42.
39. Svejstrup JQ. Mechanisms of transcription-coupled DNA repair. *Nat Rev Mol Cell Biol* 2002;3:21–9.
40. D'Incalci M, Erba E, Damia G, et al. Unique features of the mode of action of ET-743. *Oncologist* 2002;7:210–6.
41. Furuta T, Ueda T, Aune G, Sarasin A, Kraemer KH, Pommier Y. Transcription-coupled nucleotide excision repair as a determinant of cisplatin sensitivity of human cells. *Cancer Res* 2002;62:4899–902.
42. Huang H, Woo J, Alley SC, Hopkins PB. DNA-DNA interstrand cross-linking by *cis*-diamminedichloroplatinum(II): N7(dG)-to-N7(dG) cross-linking at 5'-d(GC) in synthetic oligonucleotides. *Bioorg Med Chem* 1995;3:659–69.
43. Larminat F, Zhen W, Bohr VA. Gene-specific DNA repair of interstrand cross-links induced by chemotherapeutic agents can be preferential. *J Biol Chem* 1993;268:2649–54.
44. Gajate C, An F, Mollinedo F. Differential cytostatic and apoptotic effects of ecteinascidin-743 in cancer cells: transcription-dependent cell cycle arrest and transcription-independent JNK and mitochondrial-mediated apoptosis. *J Biol Chem* 2002;26:26.
45. Mladenov E, Tsaneva I, Anachkova B. Activation of the S phase DNA damage checkpoint by mitomycin C. *J Cell Physiol* 2007;211:468–76.
46. Howlett NG, Taniguchi T, Olson S, et al. Biallelic inactivation of BRCA2 in Fanconi anemia. *Science* 2002;297:606–9.
47. Wang W. Emergence of a DNA-damage response network consisting of Fanconi anaemia and BRCA proteins. *Nat Rev Genet* 2007;8:735–48.
48. Sasaki MS. Is Fanconi's anaemia defective in a process essential to the repair of DNA cross links? *Nature* 1975;257:501–3.
49. Paz MM, Das A, Palom Y, He QY, Tomasz M. Selective activation of mitomycin A by thiols to form DNA cross-links and monoadducts: biochemical basis for the modulation of mitomycin cytotoxicity by the quinone redox potential. *J Med Chem* 2001;44:2834–42.
50. Penketh PG, Hodnick WF, Belcourt MF, Shyam K, Sherman DH, Sartorelli AC. Inhibition of DNA cross-linking by mitomycin C by peroxidase-mediated oxidation of mitomycin C hydroquinone. *J Biol Chem* 2001;276:34445–52.